10

Crystal Growth of Pharmaceuticals from Melt

J.S. Redinha[1] and A.J. Lopes Jesus[2]
[1,2]*University of Coimbra / Department of Chemistry,*
[2]*University of Coimbra / Faculty of Pharmacy,*
Portugal

1. Introduction

The preparation of crystalline powders and single crystals is an activity of utmost importance in many fields of modern industry. Single crystals are the basis of many daily necessities such as electric heaters, strain gauges, laser controllers and piezoelectric devices (Ropp 2003). In the pharmaceutical field, the search for compounds that have suitable properties to be used in drug formulation is nowadays a big challenge. In an increasingly demanding industry, science is asked to prepare crystalline forms of well defined structural patterns, with the size and shape that is required for a certain purpose. Despite recent advances in molecular modelling, it is not yet possible to accurately predict the molecular structures from our knowledge of the chemical compositions (Gdanitz 1997), which means that the study of crystal growth is still done on an experiment basis.

Crystallization is a conventional technique used to prepare solid forms. It can be carried out from solutions by decreasing temperature, solvent evaporation or by the diffusion of a much poorer solvent in solution. Alternatively, the crystalline forms can be obtained from the melt upon cooling. Unlike crystallization from solution, this does not require recovery, storage and disposal of liquids, what this means reduced environmental impact, low cost and time saving industrial processes. It therefore accomplishes the desired "green chemistry requirements". Since the pioneering work carried out in the early 1960's (Sekiguchi and Obi 1961), melt-extrusion has become an important drug delivery technology (Mollan 2003), and is currently being applied in the manufacture of a variety of dosage forms and formulations (Chokshi and Zia 2004, Breitenbach 2002, Crowley, et al. 2007, Repka, et al. 2007, Repka, et al. 2008).

Different crystals of a certain organic compound may be obtained by crystallization. These forms, called polymorphs, differ from one another by the packing and/or conformation of the molecules in a crystal lattice (Hilfiker 2006, Bernstein 2002, Threlfall 1995, Brittain 2009). Thus, polymorphs are solid forms constituted by molecules indistinguishable in gas or liquid state but exhibiting different structures in solid phase. When this difference lies just in the conformation, they are designated as conformational polymorphs (Bernstein 2002). Since the discovery that different polymorphs may have different bioavailabilities as drugs (Aguiar, et al. 1967), polymorphism has been a matter deserving great attention by pharmaceutical technology over the last half-century (Brittain 2009, Hilfiker 2006). For a given compound, only the one having the lowest Gibbs energy form is thermodynamically stable. However, in some cases, as consequence of the height of the energy barrier separating some polymorphs and the most stable one, they remain as metastable forms for a period of time long enough to be used for practical purposes as if they were stable forms (Brittain 2009).

This chapter is focused on the study of phase transitions occurring during the melt-cooling of active pharmaceutical ingredients or excipients and in the establishment of experimental conditions to obtain different kinds of solid forms. Another aim is to obtain information on the relationship between molecular and crystal structures. The compounds selected for this study were erythritol (*meso*-1,2,3,4-tetrahydroxybutane), pindolol [1-(1H-indol-4-yloxy)-3-((1-methylethyl)amino)-2-propanol], atelolol [4-(2-hydroxy-3-((1-methylethyl) amino)propoxy) -benzeneacetamide] and betaxolol hydrochloride [1-(4-(2-cyclopropylmethoxy) ethyl) phenoxy)-3-((1-methylethyl)amino)-2-propanol hydrochloride], whose structures are shown in Figure 1. Melt-growing has been frequently applied to prepare polymers (E.Donth 1992); however, very little attention has been given to compounds of smaller or medium molecular weight such as those treated in this chapter.

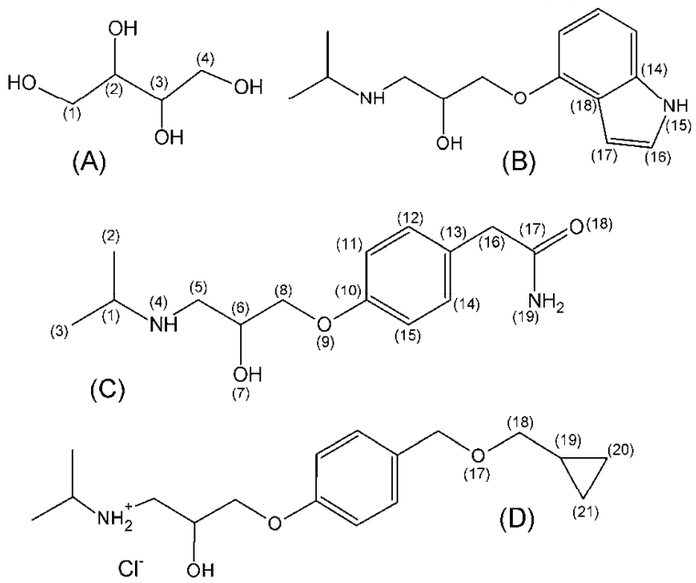

Fig. 1. Molecular structures and atom numbering of the compounds: (A) erythritol, (B) pindolol, (C) atenolol and (D) betaxolol hydrochloride. Only carbon, oxygen and nitrogen atoms are labelled. The 2-isopropylaminoethanol moiety in betaxolol and pindolol is numbered as in atenolol. In erythritol the oxygen atoms are numbered according to the carbon atom at which they are bonded.

Erythritol is widely used as a low caloric sugar. In addition, due to its sweet taste, low toxicity (Munro, et al. 1998), and high compatibility with drugs (Zhou, et al. 2000), it is an ideal excipient to be used in pharmaceutical formulations (Endo, et al. 2005, Gonnissen, et al. 2007, Ohmori, et al. 2004). The remaining compounds are used in medical practise in the treatment of hypertension and cardiovascular diseases. They belong to a group of medicines known as beta-blockers or beta-adrenergic compounds. Since betaxolol has a low solubility in water, the hydrochloride form is the most used in practise. A common feature of beta-adrenergic is the presence of the 2-isopropylaminoethanol group which enables the drug to be recognized by the characteristic centres of the biological receptors (Coulson 1994, Silverman 2004). A second moiety, varying from one compound to the other, gives some specificity to the drug. This set of compounds was selected to study the effect of various molecular features, particularly the molecular size and flexibility on the type of structures formed by crystallization.

The best quality compounds commercially available were used for this study. Attending to the effect that trace impurities may have in the crystallization process, purity of the compounds deserved great attention. Even though the compounds were labelled or certified as high purity substances, this was checked by HPLC or GC methods. A purity degree higher than 99% was found for all the original compounds. The instrumental methods used to produce the results necessary for this research program were differential scanning calorimetry (DSC), polarized light thermal microscopy (PLTM), infrared spectroscopy (IR) and X-ray or neutron diffraction.

2. Outlines of solid formation in super-cooled liquids

Before proceeding with the analysis of the results obtained for the systems under consideration, it may be useful to present an overview concerning the theoretical aspects of the formation of a solid phase from a super-cooled liquid.
When a liquid is cooled at temperatures below its freezing point, super-cooled liquid, the following phase transitions can be observed: a) precipitation of a crystalline solid; b) formation of a disordered solid (glass) which may crystallize afterwards upon heating; c) liquid-liquid separation followed by solidification of the components.

2.1 Nucleation and crystal growth

The crystallization of a homogeneous liquid phase is initiated by formation of a molecular cluster. The probability (P_n) of formation of a cluster containing n molecules more rapidly than the time derivative of the order parameter fluctuation is given by (Landau and Lifshitz 1969):

$$P_n \propto \exp\left(-\frac{\Delta G_n}{kT}\right) \tag{1}$$

where ΔG_n represents the Gibbs energy variation of the cluster formation and k the Boltzmann constant. According to the classical nucleation theory (Kelton 1991, Myerson 1999) this Gibbs energy variation has a negative and a positive contribution: the first results from the molecular aggregation and the second from the creation of the liquid/solid interface. Assuming a spherical cluster with radius r, the following expression accounting for the Gibbs energy variation can be written:

$$\Delta G_n = \frac{4}{3}\pi r^3 \Delta g + 4\pi r^2 \gamma \tag{2}$$

Δg is the Gibbs energy variation per volume unit and γ is the interfacial energy per unit area. Since $\Delta g < 0$ and $\gamma > 0$, the variation of ΔG_n with r passes through a maximum corresponding to the value of r^* given by the condition $dG_n/dr = 0$. The maximum of G_n (G_n^*) is obtained for the radius of the nucleus r^*, given by:

$$r^* = \frac{2\gamma}{|\Delta g|} \tag{3}$$

$$\Delta G_n^* = \frac{16\pi\gamma^3}{3(\Delta g)^2} \tag{4}$$

For $r < r^*$ the aggregates will dissolve into monomers because $\Delta G_n > 0$, while for $r > r^*$, $\Delta G_n < 0$ and the aggregates grow to form a crystalline phase. The molecular structure corresponding to r^* is called nucleus. The nucleation process of the new solid phase has an energy barrier height given by (4) which decreases as the super-cooling increases. In fact, the driving force for the occurrence of molecular aggregation is given approximately by $\Delta\mu=\Delta S_m \Delta T$, wherein $\Delta\mu$ is the variation of chemical potential, ΔS_m is the fusion entropy and ΔT (T_m-T, T_m is the fusion temperature) represents the super-cooling. Hence, Δg becomes more negative as ΔT increases, i.e., the energy barrier decreases as super-cooling increases. The nucleus, once formed, grows by deposition of new solid material on it. The crystal size of the material obtained by crystallization depends on the balance between nucleation and growth rates.

Thermodynamically, the temperature decrease of a super-cooled liquid favours crystal formation since the driving force of nucleation increases. However, from the kinetic point of view, crystallization becomes more difficult to occur due to viscous retardation. The maximum overall rate of crystallization is reached at a temperature for which the positive contribution given by the super-cooling equalizes the negative one arising from molecular motion (Hancock and Zografi 1997).

The nucleation just described arises by fluctuations in a homogeneous liquid phase free from any solid particles including dust and having no contact with a container. The nucleation in the presence of a solid phase (heterogeneous nucleation) has lower activation energy than the homogeneous one.

2.2 Glass transition

The metastable limit of a super-cooled liquid is sometimes not nucleation. A liquid may require such high super-cooling to crystallize that before this temperature is reached the molecules almost completely loose their translational motion. A solid is obtained by a sudden viscosity increase. This solid is amorphous because it has the short-range organization of the liquid at the temperature it was formed (glass transition temperature, T_g), but does not have the long-range order of the crystal. The glass transition is characterized by a more or less pronounced change in the derivatives of the thermodynamic properties by temperature variation (Wong and Angell 1976). For example, a sudden increase in volume and heat capacity with temperature increasing is observed. When melt-cooling is followed by DSC, the heat flow rate increases sharply as temperature decreases. Another property of a glass phase to bear in mind as background for the present work is the variation of T_g with the cooling rate. As the cooling rate increases less time is left for the molecules to adapt to the liquid structure and so higher T_g values are observed. Most glasses crystallize upon heating. At a temperature near T_g the glass devitrifies and crystallizes at a higher temperature. The DSC curve will show an increase in heat flow rate and a relaxation peak in the glass transition region, followed by an exothermic peak corresponding to crystallization.

2.3 Liquid phase separation

Another phenomenon that can occur in a super-cooled liquid before any of the transformations described above take place is liquid-liquid phase separation. This happens frequently on cooling viscous liquid mixtures (Turnbull and Bagley 1975), particularly on mixtures of polymeric materials (E.Donth 1992). As this phenomenon is observed in systems under consideration a brief note on this matter is left here.

For two miscible liquids, the variation of the Gibbs energy of mixing as a function of composition is a convex downward curve as displayed in Figure 2(a). However, for some systems a convex upward curve within a certain composition range can be observed, Figure 2(b). In this curve the points B and B′ correspond to the equilibrium phase composition or binodal composition (E.Donth 1992, Kelton 1991). The local limit of stability is given by the inflection points S and S′, whose composition is called spinodal. The mixture is unstable between S and S′ and metastable between BS and B′S′. The projection of binodal and spinodal in the T-ρ plane is shown in Figure 2(c). The maximum C is common to both curves and is called critical point. Systems with a critical point exhibit a miscible gap at temperatures below T_C. Inside the binodal nucleation of critical size particle of a certain composition and its growth *via* diffusion takes place. Inside the spinodal growth of a new phase goes *via* decomposition in which amplitude of concentration fluctuations is crucial. Liquid phase separation has also been observed for one component systems providing a long-range fluctuation alters an order-parameter of the liquid such as, for example, the density (Klein, et al. 1989, Kiselev 1999).

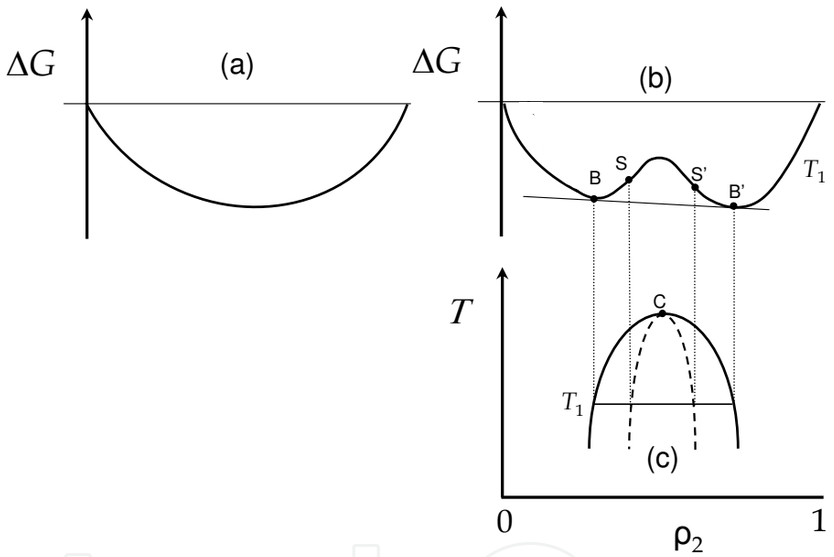

Fig. 2. Spinodal decomposition of viscous liquids: (a) Δ*G* versus density for two miscible liquids; (b) Δ*G* versus density for two partially immiscible liquid mixtures; (c) Temperature-density diagram for two partially immiscible liquid mixtures.

3. Thermodynamic information taken from DSC data

Despite being an old technique, DSC is still widely used to study the structural modifications occurring in a compound as it is cooled or heated. In the present case, it is used to investigate the phase transitions occurring in the melt-cooling process. Crystal or glass formation is observed and the phase transitions are characterized by their thermodynamic properties (temperature, enthalpy and heat capacity). Some of the structural aspects of the frozen solid can be evidenced upon heating. Hence, the following general procedure was used: samples encapsulated into aluminium pans were melted and the temperature was raised to approximately 20°C above the respective melting points.

The melt was then cooled down to approximately -160ºC at different scanning rates. The thermal cycle was completed by performing a heating run at a certain scanning rate until the melting point is reached. Apparatus and technical details of the DSC experiments can be found in previous works published by the authors (Lopes Jesus, et al., Canotilho, et al. 2010, Nunes, et al. 2004). The DSC results obtained for all compounds are summarized in Tables 1 and 2.

Compound	Cooling run	Heating run
Erythritol	Low cooling rates: crystallization T_{cryst} ≈ 14-16ºC or ≈ 40ºC ΔH_{cryst} ≈ -20 kJ mol^{-1} Higher cooling rates: glass formation Tg = -44.4 ± 0.8 ºC ; ΔCp ≈ 0.1 J mol^{-1}K^{-1}	Crystallization from glass: T_{cryst} ≈ -20 to 20ºC Fusion: *Stable polymorph* T_{fus} = 117.9 ± 0.4 ºC ΔH_{fus} = 39.4 ± 0.9 kJ mol^{-1} *Metastable polymorph* T_{fus} = 104 ± 1 ºC ΔH_{fus} ≈ 34 kJ mol^{-1}
Atenolol	Crystallization at any cooling rate: T_{cryst} = 147.1 ± 1.2 ºC ΔH_{cryst} =-36.3 ± 0.7 kJ mol^{-1}	Fusion: T_{fus} = 152.4 ± 0.5 ºC ΔH_{fus} = 36.5 ± 1.1 kJ mol^{-1}
Pindolol	Crystallization at higher temperature: T_{cryst} = 143 ± 7 ºC ΔH_{cryst} =-50± 3 kJ mol^{-1} Crystallization at lower temperature: T_{cryst} = 75.3 ± 1.1 ºC ΔH_{cryst} =-30.3 ± 1.4 kJ mol^{-1}	Crystallinity improvement of the solid formed at 75.3ºC T_{cryst} = 110 - 140ºC Fusion: T_{fus} = 169.7 ± 0.3 ºC ΔH_{fus} = 58 ± 2 kJ mol^{-1}
Betaxolol hydrochloride	Glass transition Tg ≈ -14ºC ; ΔCp ≈ 200 kJ mol^{-1}K^{-1} Tg ≈ -142ºC ; ΔCp ≈ 30 J mol^{-1}K^{-1}	Crystallization from glass: T_{cryst} = 64.4 ± 0.9 ºC ΔH_{cryst} =-23.6± 0.7 kJ mol^{-1} Fusion: T_{fus} = 113.8 ± 0.2 ºC ΔH_{fus} = 32.9 ± 1.2 kJ mol^{-1}

Table 1. Summary of the DSC data.

To obtain information concerning the thermal stability of the substances, a preliminary study was carried out in order to establish the best working conditions. It was found that atenolol and pindolol require special attention in sample preparation. During fusion, the amide group of atenolol is slowly converted into imine, which by thermal degradation gives rise to smaller molecular fragments. The degradation is substantially reduced in the absence of oxygen. Thermal oxidation of dialkylamines was observed by some authors (Dagnac, et al. 1997). To avoid degradation, the samples should be prepared in an inert atmosphere and scanning rates higher than 10ºC/min should be used in order to reduce the exposure time of the sample to high temperatures. In such conditions, no significant oxidation occurs (Esteves

de Castro and Redinha 2002). In liquid state, the indol group of pindolol is oxidized to 3-hydroxy-indol which in turn is converted into indigo (Stenlake 1979). In fact, just a few percent of degradation of pindolol is found when the sample is encapsulated in a free air atmosphere and the melt left for one hour at 160ºC. However, no degradation was detected when the samples were prepared under the conditions described for atenolol. The remaining compounds are thermally stable in the temperature interval needed for the experiments and no special precautions were taken in sampling.

A typical set of DSC curves are presented in Figures 3 and 4 for erythritol. When the compound is cooled at rates below 10ºC/min just a narrow exothermic peak corresponding to crystallization is generally observed at temperatures between 16 and 14ºC, or in a few cases at *ca*. 40ºC. At 10ºC/min, a wider crystallization peak is found at *ca*. 0ºC/min, sometimes accompanied by a glass transition at approximately -44ºC. For higher cooling rates (≥20ºC/min), only glass transition is observed. The DSC patterns show the competition between nucleation and glass transition. At low cooling rates (≤5ºC/min) only crystallization takes places, whereas for cooling rates higher than 20ºC/min the solidification gives glass. For medium values both transitions occur.

The frozen solid upon heating can melt at two different temperatures, 104 or 118ºC (most common), with enthalpies of fusion of 34 and 39 kJ mol^{-1}, respectively. In some cases, both peaks are observed simultaneously, curves (c) and (d) of Figure 4. This behaviour indicates that erythritol grown from melt may exhibit two polymorphs with the contribution of each one varying from 0 to 100%. According to the heat of fusion rule (Burger and Ramberger 1979) erythritol is a monotropic system, the higher melting point being the stable form. The solids forms obtained at medium or high cooling rates show, upon heating, devitrification followed by crystallization before fusion.

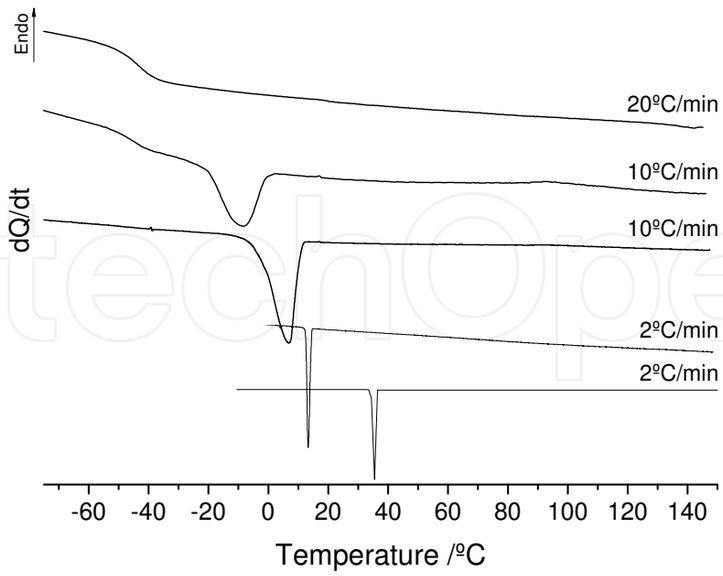

Fig. 3. DSC cooling curves of molten erythritol at different scanning rates. Reprinted from International Journal of Pharmaceutics, Vol 388, A.J. Lopes Jesus et. al. / Erythritol: Crystal growth from the melt, Page 130, Copyright (2010), with permission from Elsevier.

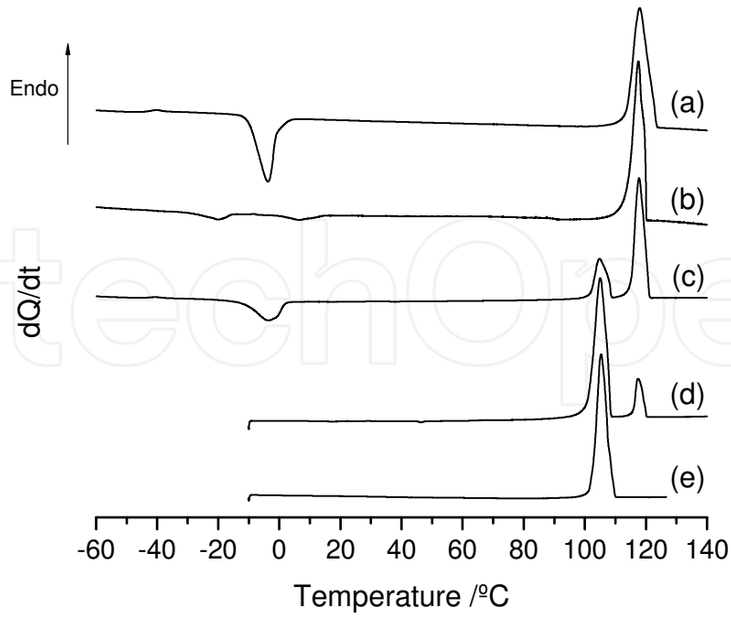

Fig. 4. DSC heating curves (10ºC/min) of solid erythritol grown from melt at 20 ºC/min (a), 10 ºC/min (b) and (c), 2 ºC/min (d) and 0.5 ºC/min (e). Reprinted from International Journal of Pharmaceutics, Vol 388, A.J. Lopes Jesus et. al. / erythritol: crystal growth from the melt, Page 131, Copyright (2010), with permission from Elsevier.

The shape of the fusion curves corresponding to the most stable form reveal that they are uncommonly asymmetric and have a large base width. This complex curve was decomposed by curve-fitting analysis using a parametric modified Gaussian function developed by Leitão *et al.* (Leitão, et al. 2002). A typical curve-fitting pattern is shown in Figure 5. A good fit was achieved using two or three individual curves, which have been characterized by their peak maximum temperatures (T_{max}). Using a *K*-means cluster analysis the values obtained for T_{max} were then grouped into different clusters. For 45 samples, three clusters were considered. The criterion used to establish the number of clusters (*K*) was that no significant decrease in the variance within each cluster was observed by increasing *K*. The following values of T_{max} were obtained: 118.5 ± 0.5 (0.18), 119.9 ± 0.4 (0.42) and 122.1 ± 0.7 (0.40). The figure in parenthesis corresponds to the probability of occurrence.

Let us now consider the thermal behaviour of the three beta-adrenergic compounds. The cooling DSC curves of molten atenolol show only a crystallization peak (~147ºC) at any scanning rate up to 100ºC/min. Therefore, when the melt-grown solid is re-heated only a fusion curve is denoted at about 152ºC. Another relevant feature evidenced by the cooling-heating cycle is the low super-cooling (5ºC) of this compound. Such a low super-cooling is not common in most organic compounds for which values as high as 100ºC can be observed.

Crystallization of pindolol occurs predominantly at 143±7ºC or 75±1ºC, with percentages of occurrence of 28 and 65%, respectively. The values of the enthalpy of crystallization are -50±3 for the first case and -30±3 kJ mol^{-1} for the second one. Sometimes, crystallization at the higher temperature is by-passed and it occurs at the much lower temperature. Samples solidified under these conditions show upon heating a slow crystallization process between 110 and 140ºC followed by another one just preceding fusion (170ºC).

Unlike the two beta-adrenergic just considered, betaxolol hydrochloride does not exhibit any crystallization peak for cooling rates down to 1º C/min; only glass transitions are observed at approximately -14 and -142ºC. In the subsequent heating process devitrification and recrystallization at ~65ºC occur, followed by fusion at 114ºC.
Following an identical procedure as that described for erythritol, the DSC fusion curves of the solid beta-adrenergic compounds after being submitted to a cooling/heating cycle were also decomposed by curve-fitting. Apparently, for all studied compounds, the solid phases obtained by crystallization from melt are mixtures of three or four unique structures (Table 2). A discussion on the origin and characterization of these structures will be given later in this chapter.

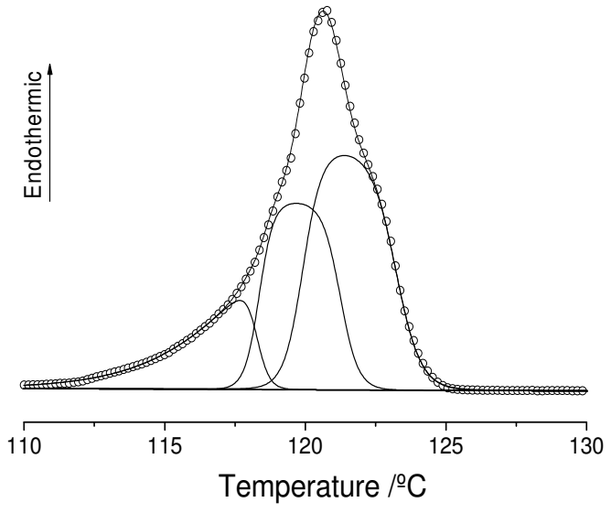

Fig. 5. Peak-fitting analysis of the fusion curve of the most stable form of erythritol. Values of T_{max} for the decomposed peaks are given in Table 2. Reprinted from International Journal of Pharmaceutics, Vol 388, A.J. Lopes Jesus et. al. / Erythritol: Crystal growth from the melt, Page 131, Copyright (2010), with permission from Elsevier.

Compound	Fusion temperatures (ºC) of the individual components of melt-grown solids after the cooling/heating cycle[a]
Erythritol	118.5 ± 0.5 (17.8) ; 119.9 ± 0.4 (42.2) ; 122.1 ± 0.7 (40.0)
Atenolol	153.0 ± 0.3 (33.3) ; 154.0 ± 0.4 (38.9) ; 155.7 ± 0.3 (27.8)
Pindolol	169.7 ± 0.2 (13.4) ; 170.2 ± 0.1 (36.1) ; 170.6 ± 0.1 (33.0) ; 171.1 ± 0.2 (17.5)
Betaxolol hydrochloride	111.3 ± 0.2 ; 112.7 ± 0.4 ; 114.2 ± 0.3 ; 115.3 ± 0.4

Table 2. Results of the curve-fitting analysis of the fusion curves for the solids crystallized from melt. [a] The figures in parenthesis correspond to the probability of occurrence.

4. Phase transitions observed by PLTM

The cooling/heating cycles previously described were observed with a polarized light microscope. This method allows a direct observation of the texture of anisotropic solids, phase transitions, existence of polymorphism, etc (Kuhnert-Brandstatter 1982). By combining PLTM with DSC, valuable information on the mechanism of phase transitions can be obtained as will be seen later in this chapter (Wiedemann and Bayer 1985).

The equipment used consists of a cell holder hot stage platform (Linkam DSC 600) coupled to a Leika DMRB microscope to which a video camera was adapted. The equipment has also a photometric absorption device which helps to follow the phase transformations taking place inside the cell. Small solid aggregates of the substance to be studied are dispersed through the bottom of the cell. The sample is then melted giving rise to small liquid drops which are then submitted to cooling/heating cycles similar to those performed in the DSC study. A few drops were observed at the same time which is an advantage since different thermal events may occur in different droplets or aggregates. Recording of the images in a computer allows a detailed study and also following the crystallization front and determining its velocity. This is valuable information regarding the mechanism of the phase transitions and of the new structures being formed.

4.1 Erythritol

Two main types of melt cooling are observed for the liquid erythritol, which are illustrated in Figures 6 and 7. For low cooling rates (Figure 6), nucleation is initiated inside a liquid drop at ~11ºC and a grained texture grows towards the surface. Fractures transversely oriented relatively to the growth direction are observed as the fresh solid phase is being deposited. The crystallization is extended to the whole liquid drop. On the subsequent heating a solid-solid transformation is generally observed at ~65ºC: the grained texture is replaced by a phase boundary texture through a diffusional process as illustrated in Figure 6(C). In this Figure the phase boundaries are indicated by arrows as eye guides. At around 120ºC, fusion takes place giving rise to a liquid with numerous air bubbles resulting from the solid fractures, Figure 6(D).

A different melt-cooling behaviour can be observed in experiments performed at 10ºC/min, which are described by the following typical example and illustrated in Figure 7: At 5ºC, crystallization is initiated on the surface of the liquid drop, progressing more rapidly along the surface than towards the interior of the liquid. At -70ºC, a crystalline shell with a grained texture encloses a glass phase resulting from vitrification of the innermost liquid. The relative amount of ordered/disordered material varies from one experiment to another. On heating, the solid particle exhibits two transformations: slow crystallization of the glass into a fine grained structure which occurs between -8 and 2ºC, followed by a solid-solid transition between 15 and 43ºC, from which a sintered particle texture results, Figure 7(C). The final solid melts at 120ºC.

In both behaviours just described the solid-solid transition corresponds to the transformation of the metastable form into the most stable one. Since no heat is involved as proved by DSC (see Figure 4), this process is fundamentally entropically driven. It is to be noted that in some experiments this transformation is not observed and the metastable phase remains unaltered until fusion (104ºC).

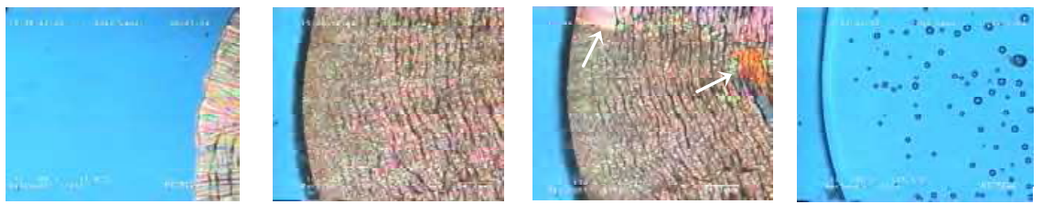

(A) (B) (C) (D)

Fig. 6. Hot-stage polarized micrographs showing the transformations occurring in erythritol as it is cooled from the melt at 2ºC/min and re-heated at 10ºC/min. Upon cooling: (A) T=11º, (B) T=-70ºC. Upon heating: (C) T=62ºC, (D) T=125ºC.

(A) (B) (C) (D)

Fig. 7. Micrographs illustrating alternative transformations of erythritol during the cooling/heating at 10ºC/min. Upon cooling: (A) T=5ºC, (B) T=-70ºC. Upon heating: (C) 20ºC, (D) T=43ºC.

In conclusion, erythritol cooled from the melt originates a crystalline metastable phase or a mixture of this phase with glassy material. On heating, three situations can occur: (a) all metastable form is converted into the stable one and just one fusion peak is observed at 118ºC; (b) the transformation is by-passed and the fusion of the metastable occurs 14ºC below; (c) only part of the metastable phase is transformed into the stable form and two fusion peaks are observed with areas depending on the relative amounts of both forms presented in the solid.

4.2 Atenolol

The crystallization of liquid atenolol is a very fast process. As super-cooling reaches a value of ~5ºC a very fast liquid/solid transformation takes place. Nucleation arises inside the liquid drops and crystallization spreads almost instantaneously all over the liquid.

4.3 Pindolol

In pindolol, the beginning of the solid formation at 143ºC is accompanied by liquid phase decomposition. As shown in Figure 8, the apparent homogeneous liquid divides into two domains just as the solid appears. The crystallization goes on in the first domain until it becomes exhausted. The second liquid domain (β) under observation crystallizes at about 70ºC. The two crystallization temperatures are in agreement with the DSC data. The textures of the solids originated by the spinodal decomposition are quite different. That obtained at higher temperature is plate-like whilst the other has a central part of fine grains surrounded by a dendrite-like texture. Keeping in mind the close structures of pindolol noted in the analysis of the fusion curves, we can conclude that the differences between these textures are linked

with the temperatures at which they are formed rather than with structural differences. In the example just referred, the liquid phases resulting from spinodal decomposition are kept far apart and therefore each one has its own crystallization temperature.

Besides the domains separated from each another by longer distances, micro-domains closer to each other arise sometimes from the liquid phase decomposition. In fact, as can be seen in Figure 9(A), the texture of the solid phase formed at higher temperature is not homogenous, highlighting the short interruptions occurring during crystallization, as can be confirmed by the plot of the velocity against time included in the Figure. In some cases, liquid-liquid separation is by-passed and the crystallization occurs at 70-75ºC exhibiting a texture of fine particles as shown in Figure 9(B).

From the results obtained from the PLTM study of pindolol crystallization the following conclusions can be drawn: crystal nucleation at higher temperature is accompanied by liquid-liquid decomposition; since it is difficult to see which phenomenon occurs first, one can conclude that these transitions take place near the critical point where the metastable region is very narrow; lower super-cooling crystallization is by-passed if decomposition does not occur or *vice-versa*: at a lower temperature the probability of nucleation is high because the metastable region between the binodal and spinodal curve is wider. As shown in the plots depicted in Figure 9, the crystallization front is an oscillating curve because the heating release of the new phase and its sequent removal from the medium disturbs the steady state conditions giving rise to super-cooling fluctuations (Jackson 1975).

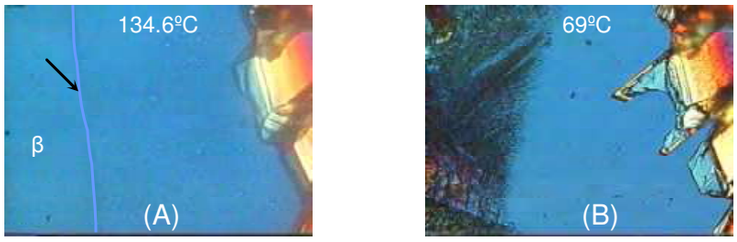

Fig. 8. Micrographs registered during cooling of pindolol from melt. (A): As crystallization is initiated, the β phase is separated out; the boundary of β is indicated in the picture by an arrow as eye guide. (B): crystallization of both domains.

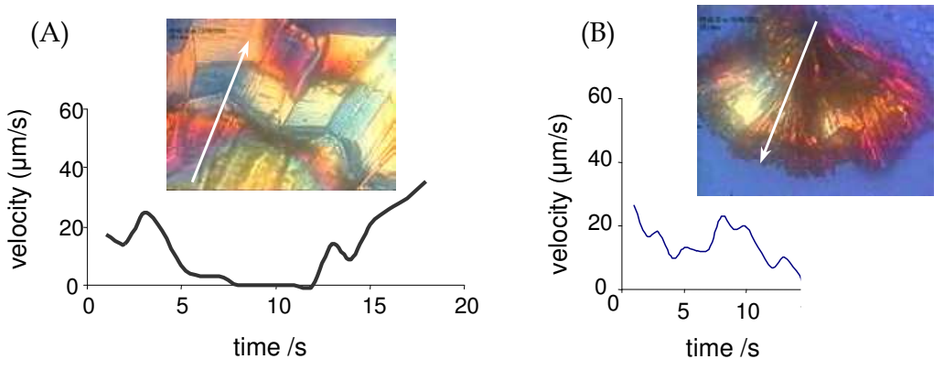

Fig. 9. (A): Texture and velocity of crystallization front for the solid grown at higher temperature. The arrow indicates the direction of front progress determinations. (B): Texture and velocity of crystallization not accompanied by liquid phase separation.

4.4 Betaxolol hydrochloride

The PLTM technique proves that betaxolol hydrochloride is manifestly the best glass former among the compounds under consideration. No crystallization is observed on cooling. Such transition is only observed on heating when the glass is frozen at a very low temperature, say -160ºC. On heating, the liquid resulting from devitrification crystallizes at 50-60ºC with slow formation of spherulites, see Figure 10. Alternatively, crystallization can occur under isothermic conditions at temperatures between 25 and 40ºC by annealing for approximately one hour. During crystallization, liquid is rejected from the solid phase and is accumulated in black-spots, which melt at about 108ºC.

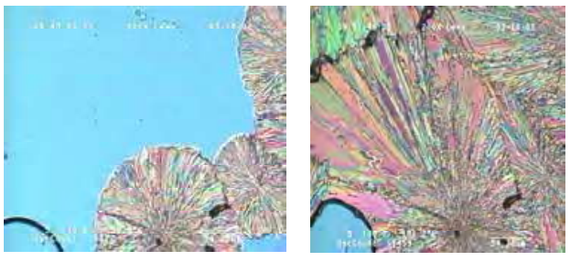

Fig. 10. Spherulites formed upon heating the melt-grown betaxolol hydrochloride.

5. Characterization of the hydrogen bond network by infrared spectroscopy

The molecules we are considering have various functional groups containing atoms able to participate in H-bonds as electron donors or acceptors. As this interaction plays a decisive role on the final structure of the solids as well as on crystallization, the knowledge of the H-bond network is indispensable to understand the melt-cooling process. We must have in mind that H-bonding is the main interaction in molecular recognition (Redinha and Lopes Jesus 2011). A hydrogen bond established between a Y atom carrying one or more electron lone-pairs and a hydrogen atom bonded to another electronegative atom (X), is generally represented as X–H···Y. As its formation weakens the X-H bond, the band maximum corresponding to its stretching vibration is displaced to lower frequencies. Another spectral manifestation of this interaction is the increase of the bandwidth and of its integrated intensity. Various methods can be used to obtain the reference spectrum of the molecule free from intermolecular hydrogen bonds (Jesus and Redinha 2009, Jesus, et al. 2003, Jesus, et al. 2006). Here, it has been calculated by applying quantum chemical methods to the monomer with the conformation exhibited in the crystalline structure.

Spectra of the compounds dispersed in a KBr pellet were registered from the melt down to -170ºC at intervals of about 5ºC during the cooling/heating cycle. The spectral region we are interested in is that between 4000 and 3000 cm^{-1}, corresponding to the OH and NH stretching vibrations. These are the vibration modes mostly affected by hydrogen bonding. The interval between 3000 and 2500 cm^{-1} is occupied by CH stretching vibrations. Due to the strong overlap of the bands in the spectral region we are considering, a peak-fit analysis is required. Good-fitts were achieved using Lorentzian functions. In this discussion we will give details of the procedure followed for erythritol while for the remaining compounds only a summary of the final results is presented.

The spectra of erythritol on cooling can be seen in Figure 11(A). The OH absorption of liquid erythritol shows a broad and symmetric band centred at ~3400cm^{-1}. As cooling is continued

the absorption band becomes asymmetric and for lower temperatures two overlapping bands are clearly distinguished. At the end of the cooling run two band components at 3346 cm^{-1} and 3243 cm^{-1} were determined as illustrated in Figure 11(A). Further spectral changes are observed on heating from -170ºC until melt is achieved, which can be followed through the band profile, Figure 11(B). Near the end of the heating process the spectrum of the solid exhibits three band components located at 3414, 3256 and 3154 cm^{-1}. A conclusion driven at once from the comparison of the spectra taken at -170 and 115ºC is that the frozen solid does not have a perfect crystalline structure and it should be heated to get to this stage. Indeed, its crystallinity has been confirmed by X-ray diffraction.

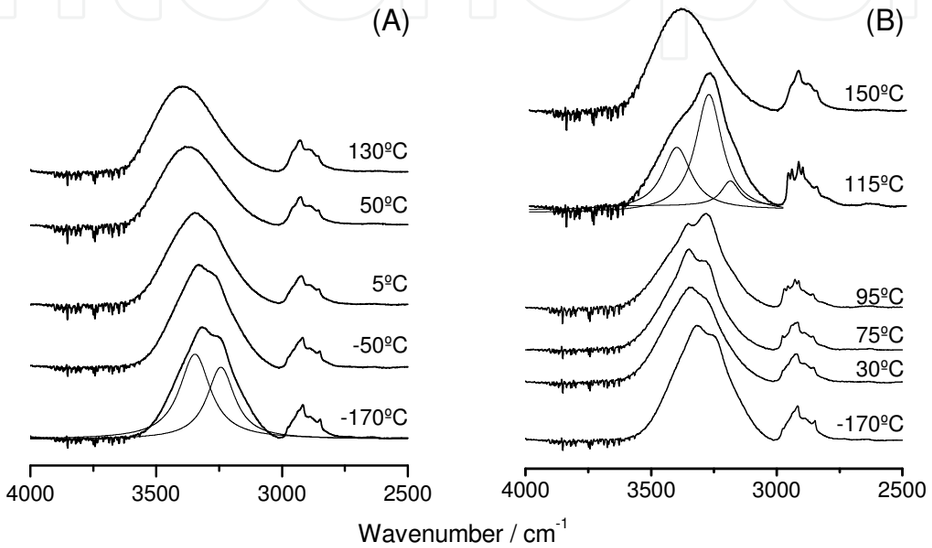

Fig. 11. Spectra of erythritol at different temperatures in the 4000-2500 cm^{-1} region during a cooling (A)/heating (B) cycle.

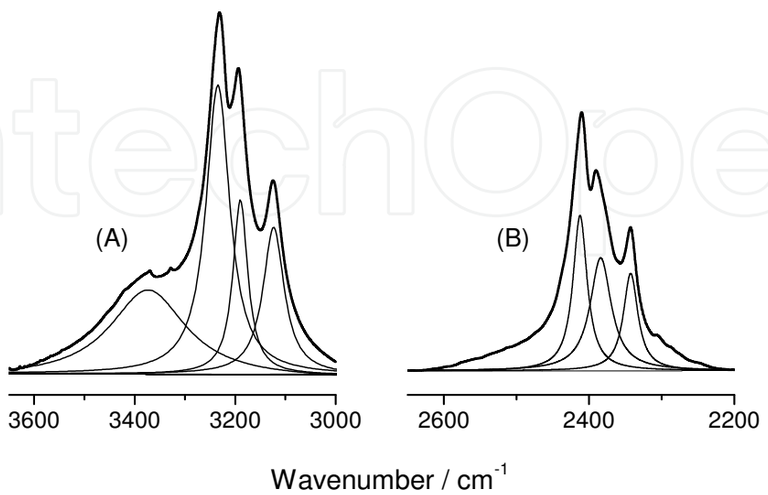

Fig. 12. Experimental spectra (bold lines) of erythritol at -258ºC in the OH (A) and OD (B) stretching regions and resolved bands (thin lines) obtained by curve-fitting.

For an accurate band identification, a spectrum of solid erythritol crystallized from water was recorded at very low temperature (-258ºC). The spectral resolution improved by lowering the temperature allows for the identification of four overlapped bands in the region under consideration as shown in Figure 12(A). Since by deuteration the band located at 3373 cm^{-1} has no counterpart in the OD region, Figure 12(B), it is not a fundamental OH stretching band but is rather a Fermi resonance. All the other absorption bands correspond to different OH stretching vibrations. It should be noted that the spectrum at this temperature differentiates the band located at 3234 cm^{-1} from that at 3190 cm^{-1}, which doesn't happen in the spectrum at 115ºC as shown in Figure 11(B).
Having identified three absorption bands as OH stretching vibrations, a step forward to their complete assignment can be made by correlating the spectral with the crystallographic data: higher values of the frequency shift correspond naturally to stronger H-bonds. Fortunately, structural data is available not only for erythritol but also for all the other compounds abridged in this study. The structural parameters of the H-bonds and the assignment of the NH and OH stretching vibrations can be found in Tables 3 and 4, respectively.

Hydrogen bond	H···Y / Å	X–H···Y / º
Erythritol		
$O_{(2)}H \cdots O_{(3)}$ or $O_{(2)}H \cdots O_{(3)}$ Conf. B	1.85	163.9
$O_{(2)}H \cdots O_{(3)}$ or $O_{(2)}H \cdots O_{(3)}$ Conf. A	1.79	164.5
$O_{(1)}H \cdots O_{(4)}$ or $O_{(4)}H \cdots O_{(1)}$	1.70	173.2
(*R*,*S*)-Atenolol		
$O_{(7)}$–H···$N_{(4)}$	2.49	119.7
$N_{(19)}$–H′···$O_{(18)}$	2.06	161.5
$N_{(19)}$–H′′···$O_{(18)}$	2.04	173.9
Pindolol		
$N_{(4)}$–H···$O_{(9)}$	2.98	106
$N_{(4)}$–H···$O_{(7)}$ (intramolecular)	2.31	114
$N_{(15)}$–H···$O_{(7)}$	2.03	156
$O_{(7)}$–H···$N_{(4)}$	1.78	172
Betaxolol hydrochloride		
$N_{(4)}^{+}$–H_A···Cl^-	2.39	137.6
$N_{(4)}^{+}$–H_B···Cl^-	2.08	175.1
O···Cl^-	3.04	–

Table 3. Structural parameters (H···A distance and X–H···Y angle) characterizing the H-bonds existing in the crystalline structures of erythritol (Ceccarelli, et al. 1980), atenolol (Esteves de Castro, et al. 2007), pindolol (Chattopadhyay, et al. 1995) and betaxolol hydrochloride (Mairesse, et al. 1984).

Various attempts have been made to correlate the frequency shift of stretching vibration (Δν) with the enthalpy of the H-bond formation (Iogansen 1999, Stolov, et al. 1996). Although the accuracy of the values calculated from these empirical correlations may vary according to the H-bond under consideration, they give an approximate indication of the strength of these interactions in energetic terms. The values of Δ*H* presented in Table 4 were estimated by the Iogansen equation (Iogansen 1999).

Compound	ν /cm^{-1}	$\Delta\nu^{a}$ / cm^{-1}	ΔH / kJ mol^{-1}	Assignment
Erythritol	3234	418	27	ν [$O_{(2)}$H] or ν [$O_{(3)}$H] Conf. B
	3190	462	28	ν [$O_{(2)}$H] or ν [$O_{(3)}$H] Conf. A
	3124	528	30	ν [$O_{(1)}$H] or ν [$O_{(4)}$H]
(*R*,*S*)-Atenolol	3459	184	18	ν (OH)
	3345	204	19	ν_{ass} (NH_2)
	3292	74	11	ν [$N_{(4)}$H]
	3160	258	21	ν_s (NH_2)
Pindolol	3404	125	15	ν [$N_{(15)}$H]
	3309	45	9	ν [$N_{(4)}$H]
	3258	330	24	ν (OH)
Betaxolol hydrochloride	3263	110	14	ν (NH_A) [b]
	3126	499	29	ν (OH)
	2791	581	31	ν (NH_B) [b]

Table 4. Assignment of the bands found in the 4000-3000 cm^{-1} region of the infrared spectra of solid erythritol, atenolol, pindolol and betaxolol hydrochloride. [a] Values of the stretching vibration of the "free" XH group were obtained from the calculated spectra of the isolated molecules adopting the crystal conformation.[b] H_A and H_B refers to the hydrogen atoms of the NH_2^+ group.

6. Crystalline ability and hydrogen bonding

As it was previously described, the melt-cooling process can originate a crystalline or glassy state depending on the cooling rate. An example of this general behaviour is that of erythritol.

In spite of the structural similitude between the beta-adrenergic compounds, they exhibit a different behaviour in the melt-cooling process as far as crystallinity is concerned. Liquid atenolol becomes solid at a low supercooling and only a crystalline form is obtained, even for high cooling rates. One can say that liquid atenolol has a good crystal making ability. At the other extreme is betaxolol hydrochloride which vitrifies on cooling at scanning rates of tenths of a degree per minute, while the crystalline phase is only obtained upon heating the frozen solid. This is an example of a good glass forming liquid. In an intermediate position between crystal and glass former is pindolol. Upon cooling, at a temperature of ~143^{o}C (26^{o}C below the melting point), a phase separation of the viscous melt occurs, accompanied by a crystallization of one of the liquid phases; the other liquid phase crystallizes partially at ~75^{o}C.

A crystal is an example of a supramolecule resulting from the self-recognition of the molecules present in the liquid (Redinha and Lopes Jesus 2011). Organic molecules such as those of the beta-adrenergic compounds have a long and flexible carbon chain (see Figure 1). In molecular terms, their packing occurs through intermolecular linking points. When these points are located at short distances the molecular fragments are constrained to occupy fixed positions and to adopt a certain conformation. The most important type of intermolecular

interaction presented in organic crystals is hydrogen bonding. The gradual directional nature of this bond, its intermediate position between a covalent and a van der Waals interaction in respect to strength, and between covalent and ionic force as far as polarity is concerned, makes this interaction to play a key role in the molecular recognition process. The H-bond network pattern is fundamental in the type of solid formed.

In Table 3 are described the H-bond networks existing in the crystalline structures of the beta-adrenergics. The different distribution of H-bonds in atenolol and betaxolol hydrochloride clearly accounts for the difference observed on cooling from the melt. In the crystalline structure of atenolol each hydrogen atom of the acetamide group is linked to the $O_{(18)}$ atom of two neighbouring molecules. In addition, the $O_{(7)}H$ group is H-bonded to $N_{(4)}$. Weak interactions involving the phenyl group, $C_{(8)}$–H···π and π···π, were also proved to exist (Esteves de Castro, et al. 2007). That is, the only part of the atenolol molecule remaining free of relatively strong intermolecular forces is the terminal isopropyl group.

Regarding the betaxolol hydrochloride, the chloride ions establishes three charged-assisted H-bonds: two with the OH and NH^+_2 groups of the same molecule and the other with the NH^+_2 group of a neighbouring molecule (see Figure 13). The molecular fragment from $C_{(6)}$ to the cyclopropyl group is not constrained by any hydrogen bond and is free to move as in the liquid phase until it got trapped due to viscosity increasing. Thus, several conformations can be adopted by this moiety.

These two examples highlight the influence of the hydrogen bonding distribution on the tendency of the compound towards either crystal or glass formation.

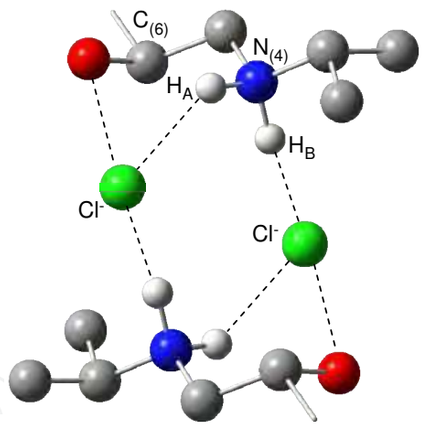

Fig. 13. Detail of the intermolecular hydrogen bonds between neighbour molecules in betaxolol hydrochloride. For better visualization some hydrogen atoms have been removed and only the molecular fragments involved in H-bonds are shown.

7. Partially disordered crystals

As it has been shown previously, the thermal methods provided evidence for the existence of more than one structure in the solids grown from melt (Table 2). Very likely, it will be rather difficult to obtain a perfect crystalline form in organic crystal of molecules of a certain size. Organic crystals may exhibit various types of imperfections in unknown amounts: vacancies in the crystal lattice, rotational or translational disorder and different orientations of the whole molecule or of some molecular fragments.

The crystalline structure of erythritol has been determined at 22.6K by neutron diffraction analysis (Ceccarelli, et al. 1980). This study reveals the existence of two conformations (A and B) (Jesus and Redinha 2009, Ceccarelli, et al. 1980), differing from each other in the positions of the two hydrogens connected to the middle oxygen atoms (see Figure 14). The occupancy percentages of the two conformations at 22.6 K are found to be 85% and 15%, respectively. Three types of hydrogen bonds have been identified: one of them is common to both conformations and connects the terminal OH groups, while the other two involve the middle OH groups of the conformations A or B, respectively (Ceccarelli, et al. 1980, Jesus and Redinha 2009). Since the existence of these two conformations does not affect the unit cell parameters, erythritol is an example of conformational isomorphism.

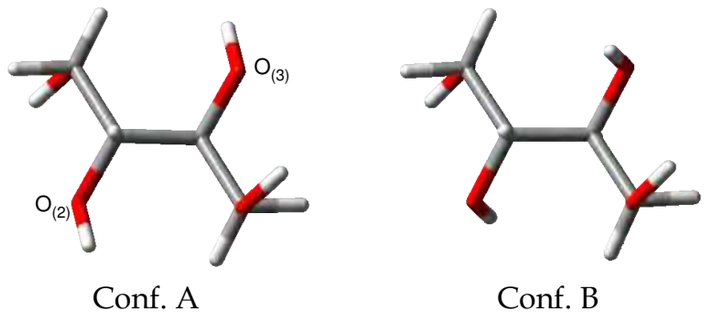

Fig. 14. Conformations of erythritol in the crystal lattice.

This situation is more complicated in the beta-adrenergic compounds. Let us consider the crystalline structures of (R,S)-atenolol and betaxolol hydrochloride. Crystals of (R,S)-atenolol of size suitable for X-ray diffraction were obtained by slow evaporation of the solvent from water-ethanol solutions. The compound crystallizes in the monoclinic crystal system (*C2/c* space group). Analysing the crystal geometry which is represented in Figure 15, three regions can be identified: the central part from $C_{(8)}$ to $C_{(16)}$ wherein the C and O atoms are in the plane defined by the benzene ring, the head consisting of the acetamide group with the C, N and O atoms in the same plane, making an angle of 81º with the central molecular backbone, and the tail extending from $C_{(6)}$ to the isopropyl group. The tail fragment exhibits two types of disorder: one is concerned with the position of the $C_{(5)}$ atom which can alternatively occupy positions 5a or 5b, Figure 15(A). The percentage occupancy of each site is 57 and 43%, respectively. Further thermal motion disorder arises from the flexibility of the tail fragment, as indicated by the ORTEP diagram given in Figure 15(B).
Betaxolol hydrochloride crystallizes in the triclinic system with P_1 symmetry (Mairesse, et al. 1984). As stated before the only detected H-bonds involve the chloride ion and the two functional groups of the molecular head. Besides these bonds, only loose van der Waals contacts occur between cyclopropyl groups. As can be seen from Figure 16(A) the structure presents disorder from $C_{(10)}$ to $C_{(19)}$. The cyclopropane group was left out of the structure refinement (Mairesse, et al. 1984). Basic betaxolol was also studied by X-ray diffraction (Canotilho, et al. 2008). This form crystallizes in the same crystal system and space group as the hydrochloride. It was found that the cyclopropylmetoxy group may acquire two alternative conformations (a and b with almost the same occupancy) resulting from the rotation around the $O_{(17)}$–$C_{(18)}$ bond as illustrated in Figure 16(B). The two cyclopropyl planes defined by each alternative conformation form an angle of 82º.

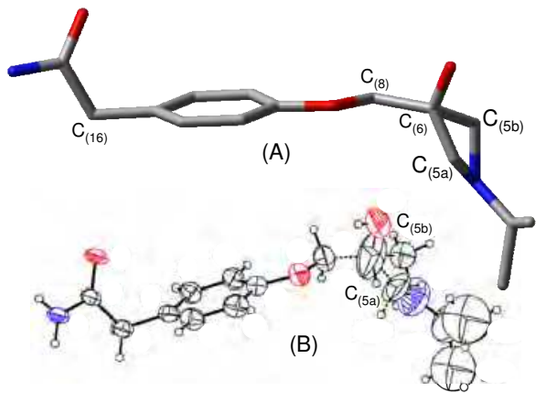

Fig. 15. (A) Geometry of (R,S)-atenolol in the crystalline structure showing the two alternative positions for the $C_{(5)}$ carbon atom; (B) ORTEP drawing (30% displacement ellipsoids) showing the thermal motion disorder exhibited by the tail fragment.

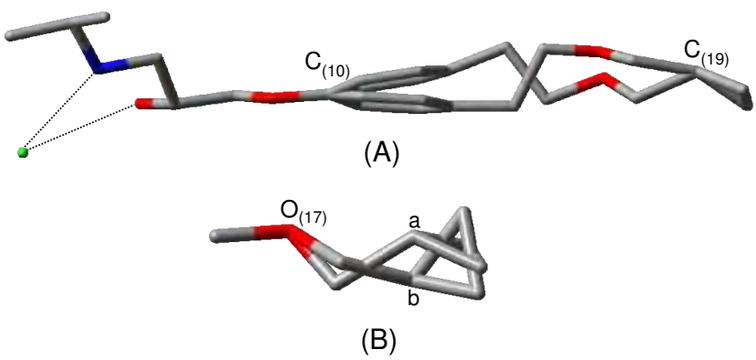

Fig. 16. (A) Geometry of betaxolol hydrochloride in the crystalline structure showing the disorder from C(10) to C(19) carbon atom; (B) two alternative conformations (a and b) adopted by the cyclopropylmetoxy group in the crystalline structure of basic betaxolol.

8. Conclusion

Grown from melt is a way to prepare solids with structures required for certain purposes. One of its greatest advantages relative to crystallization from solution is that no solvents are used. In this chapter the structure of the solid forms of compounds with pharmaceutical interest prepared in this way and the phase transitions occurring on cooling or heating were investigated. Compounds with different size and flexibility, as well as with different number and distribution of polar centres were selected for this study.

From the DSC results it was possible to conclude whether melt-cooling leads to crystalline or glassy states and to correlate the cooling rate with the crystallinity of the products obtained. In this respect it has been found that the three beta-adrenergic compounds exhibit quite distinct behaviours. To obtain crystalline compounds which produce liquids hard enough to be crystallized or just to improve the crystallinity of the solids obtained by cooling the melt, the frozen material has to be heated at a high temperature. The

thermodynamic properties determined for phase transitions by DSC are clear "windows" to understand the crystalline structures. Statistical analysis of the fusion curves proved that the molecular crystals of the compounds under study are composed of a few well-defined (single-value melting point) structures.

Visual observation of the transformations under polarized light was found to be an excellent complement to the DSC technique. The mechanisms of phase transitions involving crystalline and glassy forms upon cooling or heating could be followed by PLTM. Moreover, the melt phase separation in pindolol that sometimes accompanies melt-cooling crystallization could be studied by this technique. Athermic transitions such as the solid-solid transformation occurring in erythritol were only detected by this technique.

Hydrogen bonding plays a fundamental role in molecular recognition and consequently it is a determinant interaction from the nucleation to the final crystal. The intermolecular H-bonds were studied in all compounds during the cooling and heating processes. These interactions were detected by the infrared spectra in the stretching vibration region. Difficulty of spectra interpretation caused by the strong overlap of the stretching bands concerning the polar groups involved in H-bonding was overcome by temperature lowering, deuteration and peak-fit analysis and a detailed table of the hydrogen bonds for all compounds was presented. Moreover, the combination of spectral and structural (X-ray or neutron diffraction) data allowed a full assignment of the experimental infrared bands.

With the data obtained by the thermal and spectroscopic methods it was possible to interpret the ability of the melts to originate crystals or glassy phases upon cooling.

A conclusion deserved to be emphasized is the proof of co-existence, as a rule, of more than one structure in the organic molecular crystals. To clarify the type of such structures, X-ray and neutron diffraction data taken from the literature or obtained by the authors were used. These data point out that those organic crystals are constituted by molecules differing themselves in the orientations of the groups (case of erythritol) or with parts of well-defined structure and others with different or disordered conformations (case of beta-adrenergics). It is understandable that these partially disordered crystals can originate DSC curves showing various close melting points. This conclusion should be borne in mind by those that are interested in the study of polymorphism because it is not be reliable to consider polymorphs based solely on the value of a certain property, for example fusion temperature. Indeed, the various structural forms evidenced by the DSC fusion curves that could be considered manifestation of polymorphism are in fact consequence of crystal disordering.

9. References

Aguiar, Armando J., John Krc, Arlyn W. Kinkel, and Joseph C. Samyn. "Effect of Polymorphism on the Absorption of Chloramphenicol from Chloramphenicol Palmitate." *Journal of Pharmaceutical Sciences* 56, no. 7 (1967): 847-53.

Bernstein, Joel. *Polymorphism in Molecular Crystals*. Oxford: Oxford University Press, 2002.

Breitenbach, Jörg. "Melt Extrusion: From Process to Drug Delivery Technology." *European Journal of Pharmaceutics and Biopharmaceutics* 54, no. 2 (2002): 107-17.

Brittain, H. G., ed. *Polymorphism in Pharmaceutical Solids*. 2 ed. Vol. 192, Drugs and the Pharmaceutical Sciences. New York: Informa Healthcare USA, Inc, 2009.

Burger, A., and R. Ramberger. "On the Polymorphism of Pharmaceuticals and Other Molecular Crystals. I." *Microchimica Acta* 72, no. 3 (1979): 259-71.

Canotilho, J., R. Castro, M. Rosado, S. Nunes, M. Cruz, and J. Redinha. "Thermal Analysis and Crystallization from Melts." *Journal of Thermal Analysis and Calorimetry* 100, no. 2 (2010): 423-29.

Canotilho, João, Ricardo A. E. Castro, Mário T. S. Rosado, M. Ramos Silva, A. Matos Beja, J. A. Paixão, and J. Simões Redinha. "The Structure of Betaxolol from Single Crystal X-Ray Diffraction and Natural Bond Orbital Analysis." *Journal of Molecular Structure* 891, no. 1-3 (2008): 437-42.

Ceccarelli, C., G. A. Jeffrey, and R. K. McMullan. "A Neutron-Diffraction Refinement of the Crystal-Structure of Erythritol at 22.6 K." *Acta Crystallographica Section B-Structural Science* 36, no. DEC (1980): 3079-83.

Chattopadhyay, Tapan K., Rex A. Palmer, and Daruka Mahadevan. "Molecular and Absolute Crystal Structure of Pindolol-1-(1h-Indol-4-Yloxy)-3-[(1-Methylethyl) Amino]-2-Propanol: A Specific Beta-Adrenoreceptor Antagonist with Partial Agonist Activity." *Journal of Chemical Crystallography* 25, no. 4 (1995): 195-99.

Chokshi, Rina, and Hossein Zia. "Hot-Melt Extrusion Technique: A Review." *Iranian Journal of Pharmaceutical Research* 3 (2004): 2-16.

Coulson, Christopher J. *Molecular Mechanisms of Drug Action*. 2 ed. London: Taylor & Francis, 1994.

Crowley, Michael M., Feng Zhang, Michael A. Repka, Sridhar Thumma, Sampada B. Upadhye, Sunil Kumar Battu, James W. McGinity, and Charles Martin. "Pharmaceutical Applications of Hot-Melt Extrusion: Part I." *Drug Development and Industrial Pharmacy* 33, no. 9 (2007): 909-26.

Dagnac, Thierry, Jean-Michel Guillot, and Pierre Le Cloirec. "Investigation of the Thermal Decomposition of Selected N,N-Dialkylamides at Low Temperature." *Journal of Analytical and Applied Pyrolysis* 42, no. 1 (1997): 53-71.

E.Donth. *Relaxation and Thermodynamics in Polymers: Glass Transition*. Berlin: VCH Pub, 1992.

Endo, Kosuke, Satoko Amikawa, Asami Matsumoto, Norio Sahashi, and Satomi Onoue. "Erythritol-Based Dry Powder of Glucagon for Pulmonary Administration." *International Journal of Pharmaceutics* 290, no. 1-2 (2005): 63-71.

Esteves de Castro, R. A., João Canotilho, Rui M. Barbosa, M. Ramos Silva, A. Matos Beja, J. A. Paixão, and J. Simões Redinha. "Conformational Isomorphism of Organic Crystals: Racemic and Homochiral Atenolol." *Crystal Growth & Design* 7, no. 3 (2007): 496-500.

Esteves de Castro, R. A., and J. S. Redinha. "Unpublished Work." 2002.

Gdanitz, R. "Ab Initio Prediction of Possible Molecular Crystal Structures." In *Theoretical Aspects and Computer Modeling of the Molecular Solid State*, edited by A. Gavevezzoti. Chichester: Wiley & Sons, 1997.

Gonnissen, Y., J. P. Remon, and C. Vervaet. "Development of Directly Compressible Powders Via Co-Spray Drying." *European Journal of Pharmaceutics and Biopharmaceutics* 67, no. 1 (2007): 220-26.

Hancock, Bruno C., and George Zografi. "Characteristics and Significance of the Amorphous State in Pharmaceutical Systems." *Journal of Pharmaceutical Sciences* 86, no. 1 (1997): 1-12.

Hilfiker, Rolf, ed. *Polymorphism in the Pharmaceutical Industry*. Weinheim: Willey-VCH, 2006.

Iogansen, A. V. "Direct Proportionality of the Hydrogen Bonding Energy and the Intensification of the Stretching V(Xh) Vibration in Infrared Spectra." *Spectrochimica Acta, Part A: Molecular and Biomolecular Spectroscopy* 55, no. 7-8 (Jul 1999): 1585-612.

Jackson, K. A. "Theory of Crystal Growth." In *Treatise on Solid State Chemistry*, edited by N.B. Hannay. 50. New York: Plenum Press, 1975.

Jesus, A. J. L., M. T. S. Rosado, M. L. P. Leitão, and J. S. Redinha. "Molecular Structure of Butanediol Isomers in Gas and Liquid States: Combination of Dft Calculations and Infrared Spectroscopy Studies." *Journal of Physical Chemistry A* 107, no. 19 (May 15 2003): 3891-97.

Jesus, A. J. Lopes, and J. S. Redinha. "On the Structure of Erythritol and L-Threitol in the Solid State: An Infrared Spectroscopic Study." *Journal of Molecular Structure* 938, no. 1-3 (2009): 156-64.

Jesus, A.J.L., M.T.S. Rosado, I. Reva, R. Fausto, M.E. Eusébio, and J.S. Redinha. "Conformational Study of Monomeric 2,3-Butanediols by Matrix-Isolation Infrared Spectroscopy and Dft Calculations." *J. Phys. Chem. A* 110, no. 12 (2006): 4169-79.

Kelton, K . F . "Crystal Nucleation in Liquids and Glasses." In *Solid State Physics*, edited by H. Ehrenreich and D. Turnbull. 75–178. New York: Academic Press, 1991.

Kiselev, S. B. "Kinetic Boundary of Metastable States in Superheated and Stretched Liquids." *Physica A: Statistical Mechanics and its Applications* 269, no. 2-4 (1999): 252-68.

Klein, H., G. Schmitz, and D. Woermann. "Spinodal Decomposition in a Single-Component Fluid." *Physics Letters A* 136, no. 1-2 (1989): 73-76.

Kuhnert-Brandstatter, M. *Thermomicroscopy of Organic Compounds*. Amsterdam: Elsevier scientific publishing company, 1982.

Landau, L. D., and E.M. Lifshitz. *Statistical Physics*. Oxford: Pergamon Press, 1969.

Leitão, M., J. Canotilho, M. Cruz, J. Pereira, A. Sousa, and J. Redinha. "Study of Polymorphism from Dsc Melting Curves; Polymorphs of Terfenadine." *Journal of Thermal Analysis and Calorimetry* 68, no. 2 (2002): 397-412.

Lopes Jesus, A. J., Sandra C. C. Nunes, M. Ramos Silva, A. Matos Beja, and J. S. Redinha. "Erythritol: Crystal Growth from the Melt." *International Journal of Pharmaceutics* 388, no. 1-2 (129-35.

Mairesse, G., J. C. Boivin, D. J. Thomas, J. P. Bonte, D. Lesieur, and C. Lespagnol. "Structure Du Chlorhydrate De L'[Hydroxy-1-(R,S) Isopropylamino-2 Ethyl]-6 Dihydro-2,3 Benzoxazole-1,3 One-2, C12h16n2o3.Hcl." *Acta Crystallographica Section C* 40, no. 8 (1984): 1432-34.

Mollan, Matthew. "Historical Overview." In *Pharmaceutical Extrusion Technology (Drugs and the Pharmaceutical Sciences)*, edited by Isaac Ghebre-Sellassie and Charles Martin. New York: Marcel Dekker, Inc, 2003.

Munro, I. C., W. O. Bernt, J. F. Borzelleca, G. Flamm, B. S. Lynch, E. Kennepohl, E. A. Bär, and J. Modderman. "Erythritol: An Interpretive Summary of Biochemical, Metabolic, Toxicological and Clinical Data." *Food and Chemical Toxicology* 36, no. 12 (1998): 1139-74.

Myerson, Allan S. "Crystallization Basics." In *Molecular Modeling Applications in Crystallization*, edited by Allan S. Myerson. 55-105. New York: Cambridge University Press, 1999.

Nunes, S. C. C., M. E. Eusébio, M. L. P. Leitão, and J. S. Redinha. "Polymorphism of Pindolol, 1-(1h-Indol-4-Yloxyl)-3-Isopropylamino-Propan-2-Ol." *International Journal of Pharmaceutics* 285, no. 1-2 (2004): 13-21.

Ohmori, Shinji, Yasuo Ohno, Tadashi Makino, and Toshio Kashihara. "Characteristics of Erythritol and Formulation of a Novel Coating with Erythritol Termed Thin-Layer Sugarless Coating." *International Journal of Pharmaceutics* 278, no. 2 (2004): 447-57.

Redinha, J.S., and A.J. Lopes Jesus. "Molecular Recognition and Crystal Growth." In *Molecular Recognition: Biotechnology, Chemical Engineering and Materials Applications*, edited by Jason A. McEvoy. Chemical Engineering Methods and Technology: Novapublishers, 2011.

Repka, Michael A., Sunil Kumar Battu, Sampada B. Upadhye, Sridhar Thumma, Michael M. Crowley, Feng Zhang, Charles Martin, and James W. McGinity. "Pharmaceutical Applications of Hot-Melt Extrusion: Part Ii." *Drug Development and Industrial Pharmacy* 33, no. 10 (2007): 1043-57.

Repka, Michael A., Soumyajit Majumdar, Sunil Kumar Battu, Ramesh Srirangam, and Sampada B. Upadhye. "Applications of Hot-Melt Extrusion for Drug Delivery." *Expert Opinion on Drug Delivery* 5, no. 12 (2008): 1357-76.

Ropp, R.C. *Solid State Chemistry*. Amsterdan: Elsevier, 2003.

Sekiguchi, Keiji , and Noboru Obi. "Studies on Absorption of Eutectic Mixture. I. A Comparison of the Behavior of Eutectic Mixture of Sulfathiazole and That of Ordinary Sulfathiazole in Man." *Chemical & Pharmaceutical Bulletin* 9, no. 11 (1961): 866-72.

Silverman, Richard B. *The Organic Chemistry of Drug Design and Drug Action*. New York: Elsevier Academic Press, 2004.

Stenlake, J. B. *Foundations of Molecular Pharmacology*. Vol. 1, London: Athlone Press, 1979.

Stolov, Andrey A., Mikhail D. Borisover, and Boris N. Solomonov. "Hydrogen Bonding in Pure Base Media. Correlations between Calorimetric and Infrared Spectroscopic Data." *Journal of Physical Organic Chemistry* 9, no. 5 (1996): 241-51.

Threlfall, Terence L. "Analysis of Organic Polymorphs. A Review." *Analyst* 120, no. 10 (1995): 2435-60.

Turnbull, David, and Brain G. Bagley. "Transitions in Viscous Liquids and Glasses." In *Treatise on Solid State Chemistry*, edited by N. B. Hannay. 513-54. New York: Plenum Press, 1975.

Wiedemann, H. G., and G. Bayer. "Application of Simultaneous Thermomicroscopy/Dsc to the Study of Phase Diagrams." *Journal of Thermal Analysis and Calorimetry* 30, no. 6 (1985): 1273-81.

Wong, Joe, and C. Austen Angell. *Glass: Structure by Spectroscopy* New York Marcell Dekker, 1976.

Zhou, L. M., J. Sirithunyalug, E. Yonemochi, T. Oguchi, and K. Yamamoto. "Complex Formation between Erythritol and 4-Hexylresorcinol." *Journal of Thermal Analysis and Calorimetry* 59 (2000): 951-60.

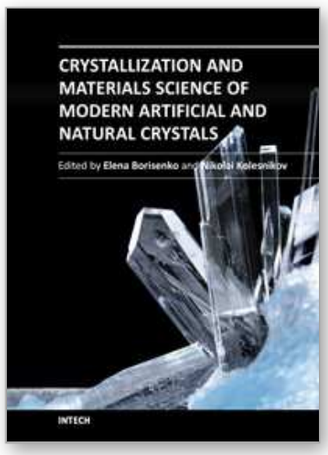

Crystallization and Materials Science of Modern Artificial and Natural Crystals

Edited by Dr. Elena Borisenko

ISBN 978-953-307-608-9
Hard cover, 328 pages
Publisher InTech
Published online 20, January, 2012
Published in print edition January, 2012

Crystal growth is an important process, which forms the basis for a wide variety of natural phenomena and engineering developments. This book provides a unique opportunity for a reader to gain knowledge about various aspects of crystal growth from advanced inorganic materials to inorganic/organic composites, it unravels some problems of molecular crystallizations and shows advances in growth of pharmaceutical crystals, it tells about biomineralization of mollusks and cryoprotection of living cells, it gives a chance to learn about statistics of chiral asymmetry in crystal structure.

How to reference

In order to correctly reference this scholarly work, feel free to copy and paste the following:

J.S. Redinha and A.J. Lopes Jesus (2012). Crystal Growth of Pharmaceuticals from Melt, Crystallization and Materials Science of Modern Artificial and Natural Crystals, Dr. Elena Borisenko (Ed.), ISBN: 978-953-307-608-9, InTech, Available from: http://www.intechopen.com/books/crystallization-and-materials-science-of-modern-artificial-and-natural-crystals/crystal-growth-of-pharmaceuticals-from-melt

INTECH
open science | open minds

InTech Europe
University Campus STeP Ri
Slavka Krautzeka 83/A
51000 Rijeka, Croatia
Phone: +385 (51) 770 447
Fax: +385 (51) 686 166
www.intechopen.com

InTech China
Unit 405, Office Block, Hotel Equatorial Shanghai
No.65, Yan An Road (West), Shanghai, 200040, China
中国上海市延安西路65号上海国际贵都大饭店办公楼405单元
Phone: +86-21-62489820
Fax: +86-21-62489821

IntechOpen